Experimental analysis of effect of orifice diameter on combustion and emission of biodiesel supercharged engine

Abstract:

In with the increasing number of automobile ownership and the increasingly stringent emission regulations, the development of clean energy has become an important issue in the field of energy and environment at present. In this paper, combustion and emission experiments of biodiesel supercharged engine were conducted to investigate the effects of orifice diameter (6×0.24mm, 6×0.35mm), engine speed (800r/min, 1400r/min), and engine load (25%, 50%, 75%, and 100%) on combustion and emission characteristics. In this paper,build a biodiesel boost injection system on the test bench, where the fuel is boosted by a high-pressure pump and injected directly through the injector via a high-pressure fuel pipe. The length of the high-pressure oil pipe is 91cm; The nozzle diameters are 6x0.24mm and 6x0.35mm, respectively, with an injection pressure of 24MPa. Real time monitoring of the pressure at the pump end and nozzle end of the fuel pipe. In the experiment, the rotational speeds of the high-pressure pump were 800r/min and 1400r/min.The results showed that for emission characteristics, at a certain rotational speed and load, the use of orifice diameter 6×0.35 mm resulted in larger carbon monoxide emission, hydrocarbon emission and carbon smoke emission and smaller NOx emission from the engine. In terms of combustion characteristics, the cylinder pressure, heat release rate, and pressure rise rate peaks are higher with orifice diameter 6×0.24mm than with orifice diameter 6×0.35mm.The pressure rise rates of both orifices have two peaks, with the first peak basically overlapping, and the orifice diameter mainly affects the second peak, and the second peak is higher with orifice diameter 6×0.24mm, and the difference is not obvious after the second peak. The cylinder pressure peak at 1400r/min is higher than the peak at 800r/min, and the peak phase is delayed. The pressure rise rate at both speeds showed a double peak, the second peak of the pressure rise rate at speed 800r/min was high and the first peak at speed 1400r/min was high.

Keywords: biodiesel; supercharged engine; orifice diameter; combustion; emission

1.Introductory

Energy, as an important material basis for the survival as well as development of human society, is the basic guarantee for the development of today's society, as well as the basic driving force for socio-economic growth [1,2]. At present, fossil energy is still the main energy source in the world. As a great gift of nature, fossil fuels take hundreds of millions of years to form naturally [3,4]. However, nowadays, with the continuous development of science and technology, the continuous growth of energy demand has led to the overconsumption of fossil energy, and the difference between fossil energy reserves and fossil energy demand is increasing year by year. Therefore, the growth of energy consumption and energy crisis is an urgent problem that needs to be solved nowadays. Nowadays, environmental problems are attracting more and more attention, which is due to the fact that economic development was strongly supported at the expense of the ecological environment before, resulting in the current environmental problems becoming more and more serious [5-7]. Many pollutants are caused by the combustion of fossil fuels, and the combustion of large amounts of fossil fuels will not only lead to increasing energy consumption, but also cause a large amount of greenhouse gases and pollutant emissions. Therefore, it is urgent to solve the environmental pollution problem [8-10].

In order to alleviate the global energy crisis and environmental pollution problems, vigorously developing renewable green resources is a topic that is being promoted all over the world. Biodiesel as a kind of green and renewable energy is also getting more and more attention [11]. Biodiesel is a biodegradable energy produced from vegetable oils or animal fats through transesterification reaction [12,13]. Its sources are very rich, and according to the 2012 report of the European Academy of Sciences Scientific Advisory Committee (EASAC), biodiesel is usually categorized into first-, second-, third-, and fourth-generation biodiesel[14,15]. Among them, the first-generation biodiesel is mainly prepared from edible oils by transesterification reaction, while the second-generation biodiesel is prepared from non-edible oils by transesterification reaction, and the third-generation biodiesel is prepared from waste edible oils by isolation, purification, and finally by transesterification reaction under acidic or alkaline conditions. The fourth generation biodiesel, on the other hand, is extracted from materials such as man-made biomass energy and is still in the basic research stage [16-20]. Biodiesel has been defined as an "environmentally friendly fuel" due to its unique advantages of being degradable, low-emission, carbon-neutral, and non-toxic, and is currently the most likely alternative to fossil diesel [21,22]. Many researchers [23-26] have also shown that the physicochemical properties of biodiesel are very close to those of diesel. The advantages of biodiesel applied to diesel engines are very obvious, which can be shown as follows: (1) Biodiesel can be directly applied to diesel engines without modifications to the fuel supply and fuel injection system [27,28]. (2) Compared with diesel fuel, biodiesel has a higher cetane number and is free of aromatics, with an oxygen content of about 10-11%. These properties of biodiesel can promote adequate

fuel combustion while significantly reducing the emission of toxic pollutants in the engine exhaust [29]. (3) Biodiesel has good lubricating properties. Since the kinematic viscosity of biodiesel is greater than that of traditional fossil diesel, it has better lubrication properties, which results in reduced friction losses during engine operation, smoother engine operation, and increased engine service life [30]. (4) Biodiesel possesses a higher flash point and freezing point than diesel, indicating that biodiesel is less likely to explode, so biodiesel is safer than ordinary diesel in transportation, storage and application [31].

In this paper, combustion and emission experiments of biodiesel supercharged engine were carried out to investigate the effects of orifice diameter, speed and load on combustion and emission characteristics.

2. Materials and Methods

2.1 The fuel used in the experiments of this thesis is biodiesel. Its physical and chemical properties are shown in Table 1 below.

Table 1 Physical and chemical properties of biodiesel

Fuel type / Physical and chemical properties	biodiesel
Density (g/cm3;20□)	0.875
Kinematic viscosity(mm2/s;40□)	4.185
Surface Tension(kg/s2;40□)	0.028
Cetane number	56

2.2 The test setup and related parameters of the engine are as follows:

Table 2 Technical parameters of biodiesel supercharged engines

Name	Type and main parameters
Type	Six-cylinder, four-stroke, supercharged, intercooled
Bore/Stroke/mm	114/135
Compression ratio	18：1
Total Displacement/L	8.27
Speed/r·min^{-1}	800 1400
Rated power/KW	184
Oil supply advance angle/0 ° CA BTDC	6
Nozzle diameter/mm	6x0.24 6x0.35
Starting pressure/MPa	19

Table 3 Main instrumentation used in the test

Instrumentation	Manufacturer and Model
Extinction Smoke Meter	AVL Corporation, 439 Opacimeter Matte Smoke Meter
Gas Emission Analyzer	AVL Corporation, AVLCEB serials
Measuring and Control Instruments	Eico Electro-Mechanical Corporation, EIM301D
Dynamometers	Eico Electro-Mechanical Corporation, PECD9400
Cylinder Pressure Sensor	Kistler Corporation, 6125B
Charge Amplifier	Kistler Corporation, 5015
Data Acquisition Instruments	Yokogama Corporation, DL750
Electronic balances	Shenyang Tenglong Electronics Co,ES1000k × 1

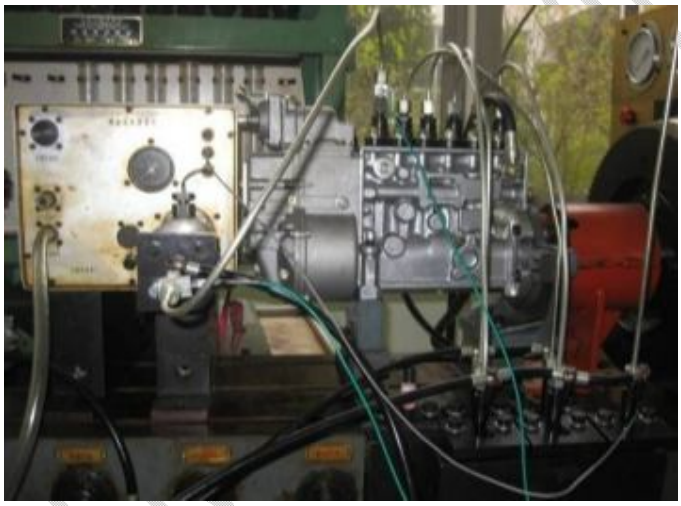

Figure 1. Picture of engine test setup

3. Results and Discussions

3.1 Effects of different orifice diameters on biodiesel supercharged engine emissions

In this paper, we study the emission pattern of CO emission, HC emission, NOx emission and carbon smoke emission of the supercharged engine under four loads, two speeds and two orifice diameters. In the experiment, the size of the orifice diameter was taken as 6×0.24mm and 6×0.35mm respectively, and the size of the load was taken as 25%, 50%, 75% and 100% respectively, and Excel software was used to make the relevant experimental data into line graphs, compare and analyze the differences, and draw relevant conclusions.

3.1.1 Effect of supercharged engine orifice diameter on CO emission

Figure 2 shows the speed of 1400r/min, two different orifice diameter (6 × 0.24mm, 6 × 0.35mm) in four different loads (25%, 50%, 75%, 100%) under the working conditions, the change rule of CO emissions. First of all, analyze the folding line of the orifice diameter of 6×0.24mm: CO emission

decreases with the increase of load first and then tends to stabilize, in the load of 25%-75%, CO emission decreases with the increase of load, and reaches the minimum emission of 33.21 ppm when the load is 75%; when the load is 75%-100%, CO emission remains basically unchanged. At 75%-100% load, the CO emission remained basically unchanged. Analyzing the folded line with the orifice diameter of 6×0.35mm: the CO emission increases with the increase of load, and keeps the same increase between 25% and 75% of the load, and increases more after 75% of the load, and reaches the maximum emission of 627.2ppm at 100% of the load. comparing the analysis of the two folded lines, no matter how the load is changed, the CO emission of the orifice diameter of 6×0.35mm is the lowest, and the CO emission of the orifice diameter of 6×0.35mm is the lowest, and the CO emission is the highest. × 0.35 mm is always larger than that of 6 × 0.24 mm, and the difference between the CO emissions of the two orifice diameters increases gradually with the increase of load.

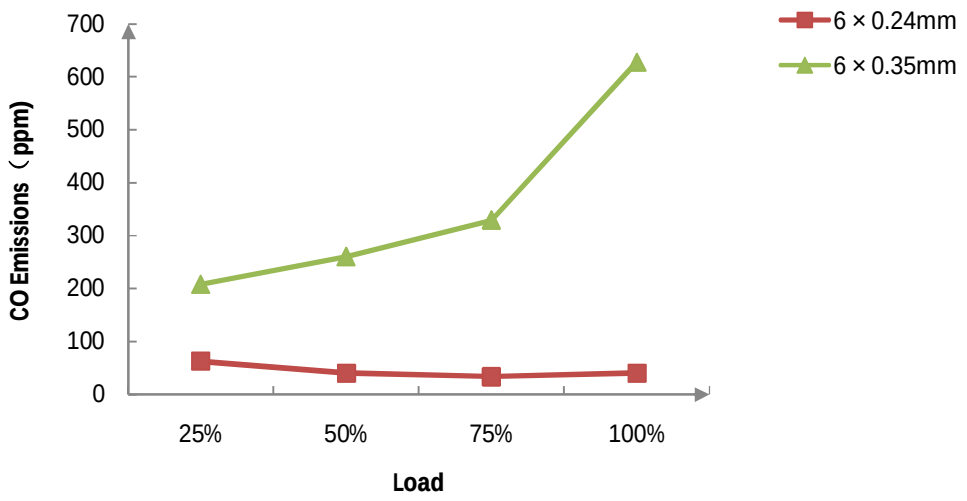

Figure 2. CO emissions for different orifice diameters

3.1.2 Effect of supercharged engine orifice diameter on HC emissions

Figure 3 shows the change rule of HC emission under four loads (25%, 50%, 75%, 100%) with the speed of 1400r/min and two different orifice diameters (6 × 0.24mm, 6 × 0.35mm). First of all, analyze the folding line of the orifice diameter of 6 × 0.24mm: HC emission does not change significantly with the increase of load, and remains stable, and the overall emission is around 14ppm. Analyze the line with orifice diameter of 6 × 0.35mm: HC emission increases with the increase of load, and it grows slowly when the load is 25%-75%, but HC emission increases rapidly after 75% load, and it reaches the maximum value of 155.88ppm when the load is 100%. two line graphs have no intersection, and the HC emission of the line with orifice diameter of 6 × 0.35mm is always larger than that of the line with orifice diameter of 6 × 0.35mm. The two line graphs always have no intersection point, and the HC emission of the orifice diameter of 6 × 0.35mm is always larger than the HC emission of the orifice diameter of 6 × 0.24mm, and the difference gradually increases.

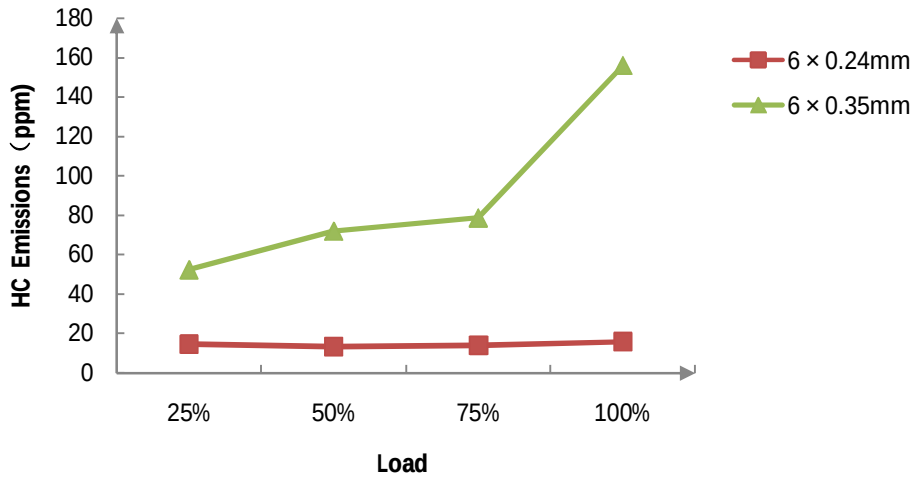

Figure 3. HC emissions under different loads

3.1.3 Effect of supercharged engine orifice diameter on NOx emission

Figure 4 shows the rotational speed of 800r/min, two different orifice diameters (6 × 0.24mm, 6 × 0.35mm) in four kinds of load (25%, 50%, 75%, 100%) under the working condition, NOx emission rule of change. Firstly, analyze the folding line with orifice diameter of 6 × 0.24mm: NOx emission increases with the increase of load, the minimum emission is 461.34ppm, and the maximum emission is 1415.21ppm. Analyze the folding line with orifice diameter of 6 × 0.35mm: NOx emission increases with the increase of load and then tends to stabilize, and NOx emission changes with the increase of load at the loads of 25%-75%. At 75%, the NOx emission increases with the increase of load, and the maximum emission is 816.9ppm. At 75%-100%, the NOx emission is almost unchanged. Comparison of the two folding lines: the two folding lines have no intersection point, the folding line of the orifice diameter of 6 × 0.24mm is always above the folding line of the orifice diameter of 6 × 0.35mm, i.e., under the same load, the NOx emission of the orifice diameter of 6 × 0.24mm is always greater than that of the orifice diameter of 6 × 0.35mm, and the difference of the NOx emission of the two orifice diameters is gradually increasing.

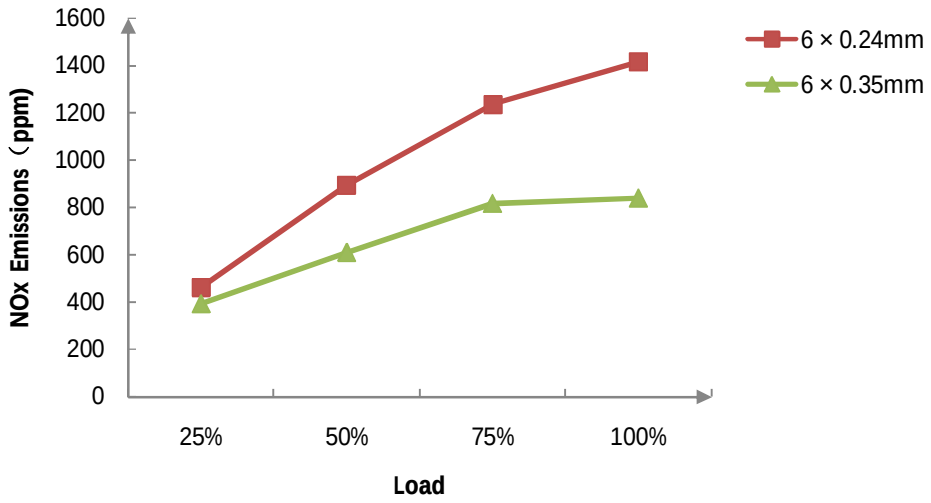

Figure 4. NOx Emissions from Different Orifice Diameters

Figure 5. shows the change rule of NOx emission under four loads (25%, 50%, 75%, 100%) at a speed of 1400r/min with two different orifice diameters (6 × 0.24mm, 6 × 0.35mm). The NOx emissions of both orifice diameters increase with the increase of load, and the maximum NOx emissions of the orifice diameter of 6 × 0.24mm is 1266.3 ppm, and the maximum NOx emissions of the orifice diameter of 6 × 0.35mm is 949.4 ppm. comparing the two folding lines, we analyze that: there is no intersection between the two folding lines, and the folding line of the orifice diameter of 6 × 0.24mm always lies in the middle of the orifice diameter of 6 × 0.35mm, and the folding line of the orifice diameter of 6 × 0.24mm always lies in the middle of the orifice diameter of 6 × 0.35mm. The line with a diameter of 6 × 0.35mm is always above the line with a diameter of 6 × 0.35mm, i.e., under the same load, the NOx emission of 6 × 0.24mm is always greater than the NOx emission of 6 × 0.35mm.

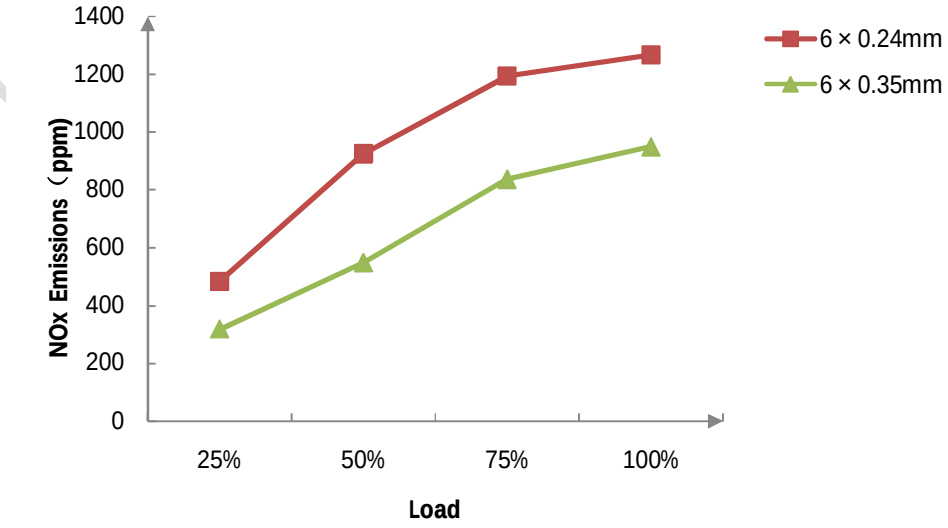

Figure 5. NOx Emissions from Different Orifice Diameters

3.1.4 Effect of supercharged engine orifice diameter on carbon smoke emission

Figure 6. shows the rotational speed of 800r/min, two different orifice diameters (6×0.24mm, 6×0.35mm) in four kinds of load (25%, 50%, 75%, 100%) under the working condition, the change rule of carbon smoke emissions. Firstly, analyze the line graph of the orifice diameter of 6×0.24mm: the carbon smoke emission does not change obviously with the increase of load, the carbon smoke emission is low, the change range is between 0.01m-1-0.04m-1, most of the carbon smoke emission under load is around 0.01m-1, the maximum value is only 0.039m-1. Analyze the line graph of the orifice diameter of 6×0.35mm. 0.35mm: the carbon smoke emission increases with the increase of load, and the increase of carbon smoke emission increases gradually with the increase of load, and reaches the maximum emission of carbon smoke when the load is 100%, with the value of 2.063m-1. Compare the analysis of two folding lines: there is no intersection between two folding lines, and the folding line of the diameter of the orifice of 6×0.35mm is always above the folding line of the diameter of the orifice of 6×0.24mm, i.e., under the same load, the emission of carbon smoke is only about 0.01m-1, with the maximum value of 0.039m-1. That is to say, under the same load, the emission of carbon smoke from the 6×0.35mm diameter orifice is always greater than that from the 6×0.24mm diameter orifice.

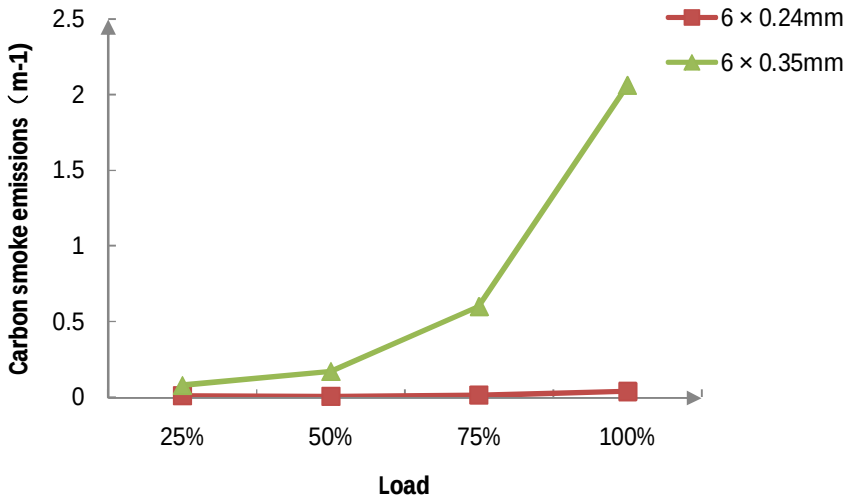

Figure 6. Carbon Smoke Emission from Different Orifice Diameters

Figure 7 shows the rotational speed of 1400r/min, two different orifice diameters (6 × 0.24mm, 6 × 0.35mm) in the four load (25%, 50%, 75%, 100%) under the working conditions, the change rule of carbon smoke emissions. Two kinds of orifice diameter carbon smoke emissions are increased with the increase of load, orifice diameter of 6 × 0.24mm carbon smoke emissions of the minimum value of 0.02m-1, the maximum value of 0.064m-1, the increase is small. The minimum value of carbon smoke emission of 6×0.35mm diameter is 0.309m-1, and the maximum value is 0.643m-1, which is a relatively large increase. The minimum carbon smoke emission of 0.309m-1 for 6×0.35mm is still larger than the maximum emission of 0.064m-1 for 6×0.24mm, with a significant difference, indicating that no matter how the load is

changed, the carbon smoke emission of 6×0.35mm is always larger than the carbon smoke emission of 6×0.24mm.

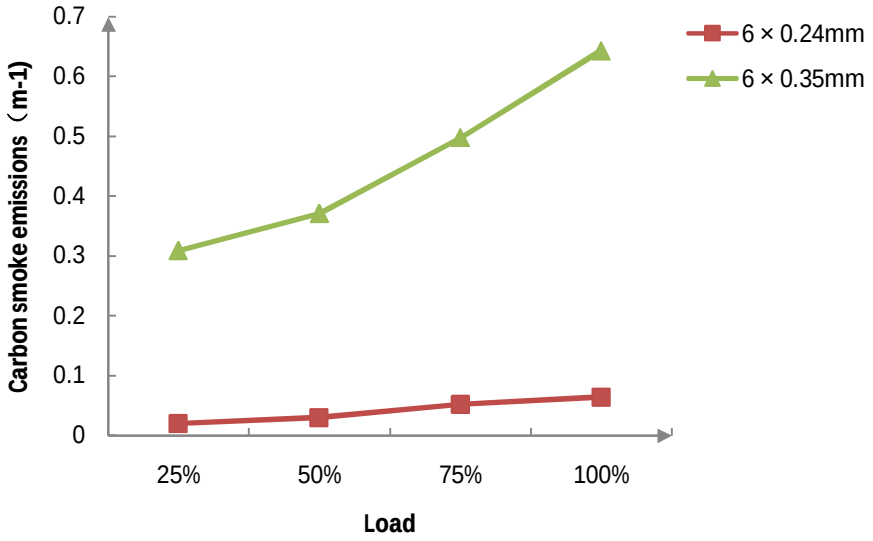

Figure 7. Nozzle Diameter Carbon Smoke Emissions

3.2 Effect of different speeds and orifice diameters on combustion in supercharged engines

In the nozzle diameter of a certain, different crankshaft angle conditions, comparative analysis of the engine speed on the cylinder pressure, pressure rise rate of the impact. The nozzle diameter is 6 × 0.24mm, the crankshaft angle is selected in the range of -30 ° CA-40 ° CA to study the effect of rotational speed on cylinder pressure, and the crankshaft angle is selected in the range of -73 ° CA-120 ° CA to study the effect of rotational speed on the rate of pressure rise.

Under a certain rotational speed and a variety of crankshaft angle conditions, the effects of different orifice diameters on cylinder pressure, heat release rate and pressure rise rate were comparatively analyzed. The rotational speed is 1400r/min, the diameter of the nozzle is 6 × 0.24mm, 6 × 0.35mm, the crankshaft angle is selected in the range of -30 ° CA-40 ° CA to study the effect of different nozzle diameters on the cylinder pressure, and the crankshaft angle is selected in the range of -30 ° CA-60 ° CA to study the effect of different nozzle diameters on the rate of exothermic heat. -The crankshaft angle was selected in the range of -73 ° CA-120 ° CA to study the effect of orifice diameter on the rate of pressure rise.

3.2.1 Effect of supercharged engine speed on cylinder pressure

Figure 8 shows the cylinder pressure graph for 100% load, the diameter of the spray hole is 6 × 0.24mm, and the crankshaft turning angle is between -30 ° CA-40 ° CA. First of all, analyze the curve of 800r/min: from the starting point, the cylinder pressure increases and then decreases with the increase of the crankshaft angle, and the cylinder pressure reaches the peak when the crankshaft angle is 8 ° CA, and the maximum cylinder pressure is 9.18784Mpa. analyze the curve of 1400r/min: from the starting point, the cylinder pressure increases and then decreases with the increase of the crankshaft angle, and the cylinder pressure reaches the peak when the crankshaft

angle is 14.5 ° CA, and the cylinder pressure increases and then decreases with the increase of the crankshaft angle. Analyze the curve of 1400r/min: from the starting point, the cylinder pressure increases and then decreases with the increase of crankshaft angle, and the cylinder pressure reaches a peak at the crankshaft angle of 1400r/min, and the maximum cylinder pressure is 12.50967Mpa. Compare the analysis of the two curves: the cylinder pressure reaches a peak at the speed of 800r/min and the peak at the speed of 1400r/min earlier than the peak at the speed of 1400r/min, and the peak value of the speed of 1400r/min is large, and there is no intersection of the two curves. At the same crankshaft angle, the cylinder pressure at 1400r/min is always greater than that at 800r/min.

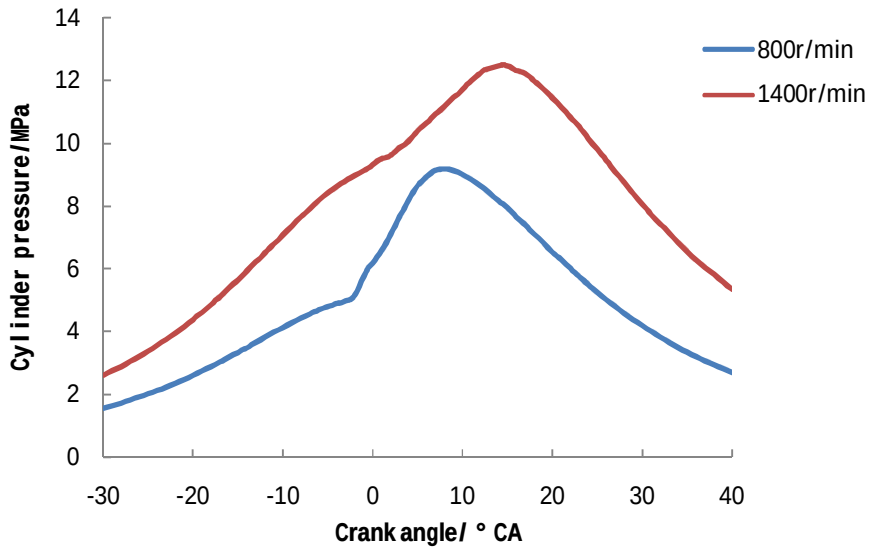

Figure 8. Cylinder pressure at different speeds

3.2.2 Effect of supercharged engine speed on the rate of pressure rise

Figure 9 represents the cylinder pressure graph for a 100% load, a spray hole diameter of 6 x 0.24 mm, and a crankshaft turn angle between -30°CA and 40°CA. Firstly, analyze the curve for a speed of 800 r/min: at crankshaft rotation angles of -40°CA --13.5°CA, -3.5°CA-1°CA, 0.5°CA-3°CA, 19.5°CA-40°CA, the The rate of pressure rise increases with increasing crankshaft angle; the rate of pressure rise decreases with increasing crankshaft angle for crankshaft angles of -13.5°CA - 3.5°CA, -1°CA - 0.5°CA, 3°CA - 19.5°CA. The maximum pressure increase rate is 0.61906Mpa/°CA at -1°CA, and the minimum pressure increase rate is -0.32424Mpa/°CA at 19.5°CA. Analyzing the curves at 1400r/min: the crankshaft angle decreases at -40°CA --10°CA, 2°CA --9.5°CA, 3°CA -19.5°CA, and 3°CA -19.5°CA, respectively. -9.5°CA, 24.5°CA-40°CA, the rate of pressure rise increases with the increase of crankshaft angle; crankshaft angle at -10°CA-2°CA, 9.5°CA-24.5°CA, the rate of pressure rise increases with the increase of crankshaft angle. crankshaft rotation angle increases. The maximum pressure increase rate is 0.32Mpa/°CA when the crankshaft angle is -10°CA, and the minimum pressure increase rate is -0.37624Mpa/°CA when the crankshaft angle is 24.5°CA. Comparing the two curves, the maximum pressure increase rate is large at 800r/min, and the minimum pressure increase rate is small at 1400r/min, and there are three intersection points between the two curves. There are three intersection points between the two

curves. When the crankshaft angle is -2 ° CA-7 ° CA, 20.5 ° CA-40 ° CA, the pressure increase rate of the speed of 800r/min is large; when the crankshaft angle is -40 ° CA-2 ° CA, 7 ° CA-20.5 ° CA, the pressure increase rate of the speed of 1400r/min is large. The rate of pressure rise is large for a speed of 1400r/min.

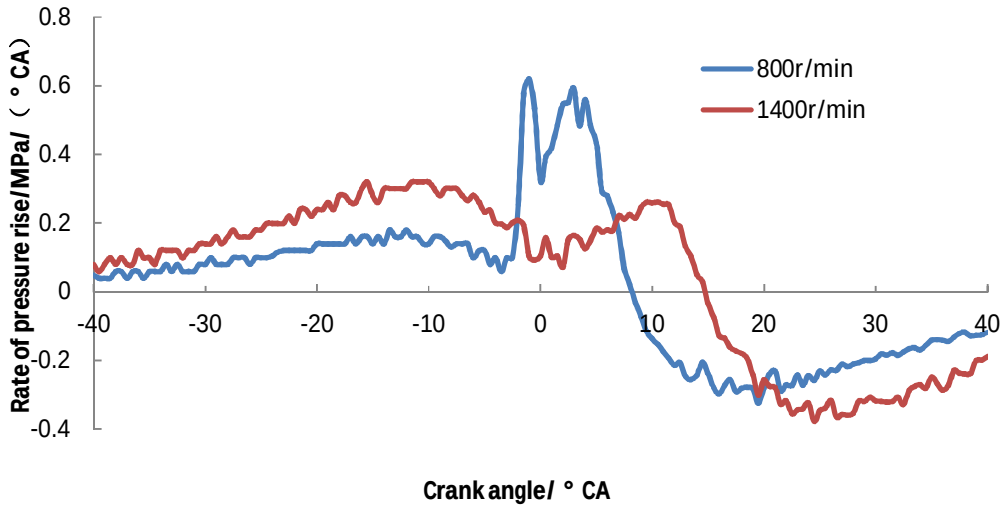

Figure 9. Pressure Rise Rates at Different Rotation Speeds

3.2.3 Effect of different orifice diameters on cylinder pressure in supercharged engines

Figure 10 represents the cylinder pressure graph for 100% load, speed of 1400r/min, and crankshaft turning angle between -30°CA and 40°CA. First of all, analyze the nozzle diameter of 6 × 0.24mm curve: from the starting point, the cylinder pressure with the increase in crankshaft angle increases first and then decreases, in the crankshaft angle is 14.5 ° CA when the cylinder pressure reaches the peak, at this time, the maximum cylinder pressure is 12.50967Mpa. analyze the curve of the diameter of the nozzle hole of 6 × 0.35mm: from the starting point, the cylinder pressure with the increase in the crankshaft angle first and then decreases, at the crankshaft angle is -30 ° CA - 40 ° CA between the cylinder pressure graphs. Analyze the curve of 6×0.35mm: from the starting point, the cylinder pressure increases with the increase of crankshaft angle, then decreases, and the cylinder pressure reaches the peak when the crankshaft angle is 14.5°CA, and the maximum cylinder pressure is 12.30029Mpa. Compare and analyze the two curves: the diameter of the nozzle hole is 6×0.24mm and the diameter of the nozzle hole is 6×0.35mm reach the peak at the same time, and the maximum cylinder pressure is close to each other. Before the peak, the crankshaft angle of 4 ° CA before the nozzle diameter of 6 × 0.35mm cylinder pressure is higher than the nozzle diameter of 6 × 0.24mm cylinder pressure, crankshaft angle of 4 ° CA after the two kinds of nozzle diameter of the cylinder pressure trend remains the same, in the vicinity of the peak cylinder pressure there is a slight difference.

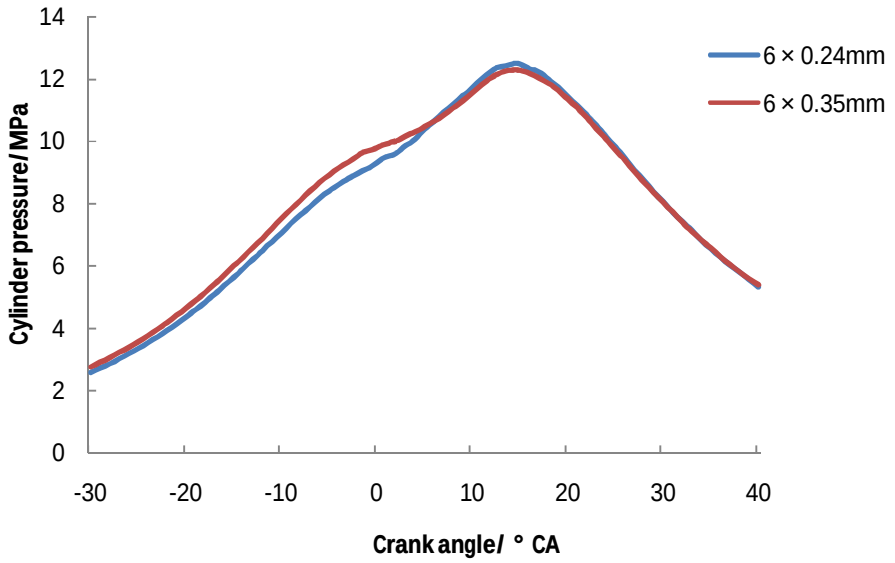

Figure 10. Cylinder Pressure for Different Orifice Diameters

3.2.4 Effect of different orifice diameters on exothermic rate of supercharged engine

Figure 11 shows the scatter plot of the exothermic rate for 100% load, speed of 1400r/min, and crankshaft angle between -30°CA-60°CA. First of all, analyze the curve of the nozzle diameter of 6×0.24mm: from the starting point, the exothermic rate increases and then decreases with the increase of the crankshaft angle, the exothermic rate reaches the peak when the crankshaft angle is 11.5°CA, at this time, the maximum pressure of the cylinder, the value of 241.92Mpa. analyze the curve of the nozzle diameter of 6×0.35mm: from the starting point, the exothermic rate increases and then decreases with the increase of crankshaft angle, at the crankshaft angle of 12°CA, the exothermic rate reaches the peak when the crankshaft angle is 12°CA. In the crankshaft angle is 12.5 ° CA when the cylinder pressure peaks, this time the cylinder pressure is maximum, the value of 231.504Mpa. Comparison of the two curves: nozzle diameter of 6 × 0.24mm to reach the peak than the diameter of the nozzle hole of 6 × 0.35mm to reach the peak earlier than the 1 ° CA, the maximum exothermic rate of the diameter of the nozzle hole of 6 × 0.24mm is high, the value of the difference is 10.416 At crankshaft angles of -30°CA-1.5°CA and -14°CA-25.5°CA, the exothermic rates of the two orifice diameters are almost the same, and the exothermic rate of the orifice diameter of 6×0.24mm is high at the crankshaft angles of -1.5°CA-14°CA, with a difference of 10.416 MPa. The exothermic rate of 6×0.35mm in diameter of the spray hole is high when the crankshaft angle is 25.5°CA-60°CA, and the exothermic rate is high when the crankshaft angle is -1.5°CA-14°CA.

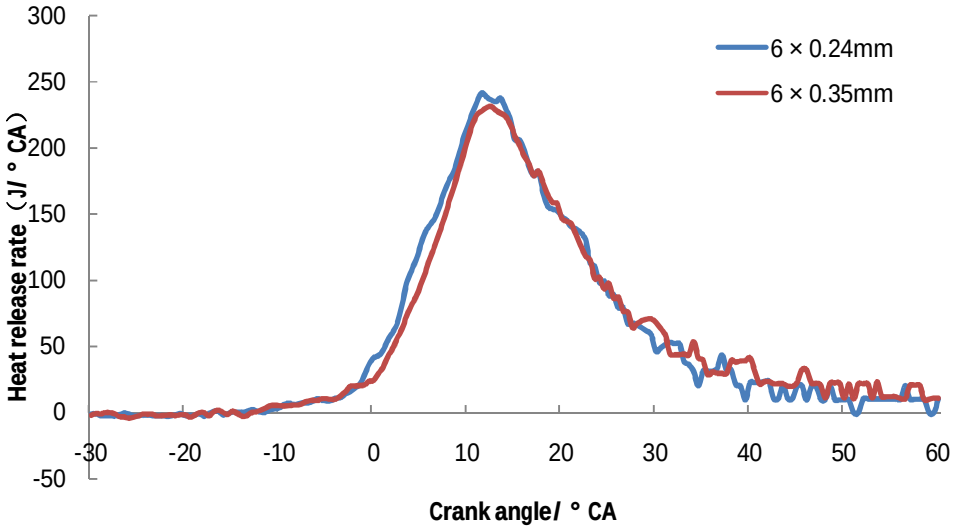

Figure 11. Heat release rate for different hole diameters

3.2.5 Effect of different orifice diameters on the rate of pressure rise in supercharged engines

Figures 12 represent the scatter plot of the exothermic rate for 100% load, speed of 1400 r/min, and crankshaft turning angle between -30°CA and 60°CA. The exothermic rate at two different orifice diameters increases and then decreases with the crank angle, increases again and then decreases, and continues to increase after reaching the minimum exothermic rate. The rate of pressure rise increases with the increase of crank angle at -40°CA --10°CA, 2°CA - 9.5°CA, 24.5°CA-40°CA; crank angle at -10°CA-2°CA, 9.5°CA-24.5°CA, the rate of pressure rise decreases with the increase of crankshaft angle. The crankshaft angle of -10°CA is the peak of the nozzle diameter of 6×0.35mm, and the pressure rise rate is the largest at this time, with a value of 0.32MPa/°CA, and the crankshaft angle of 24.5°CA is the other peak of the nozzle diameter of 6×0.35mm, and the pressure rise rate is the smallest at this time, with a value of -0.37624MPa/°CA. The crankshaft angle of 11.5°CA is the peak of the nozzle diameter of 6×0.35mm, and the pressure rise rate is the smallest at this time, with a value of -0.37624MPa/°CA. The crankshaft angle of 11.5°CA is the peak of the orifice diameter of 6×0.24mm, and the pressure rise rate is maximum at this time, with a value of 0.32592MPa/°CA, and the crankshaft angle of 24°CA is the peak of the orifice diameter of 6×0.24mm, and the pressure rise rate is minimum at this time, with a value of -0.39654MPa/°CA. The pressure rise rate of the two curves in the crankshaft angle of -1°CA The difference between the two curves in the crankshaft angle of -1°CA and -11.5°CA is the most obvious, the fluctuation of the pressure rise rate of the orifice diameter of 6×0.24mm is more drastic, and the fluctuation of the pressure rise rate of the orifice diameter of 6×0.35mm is more balanced.

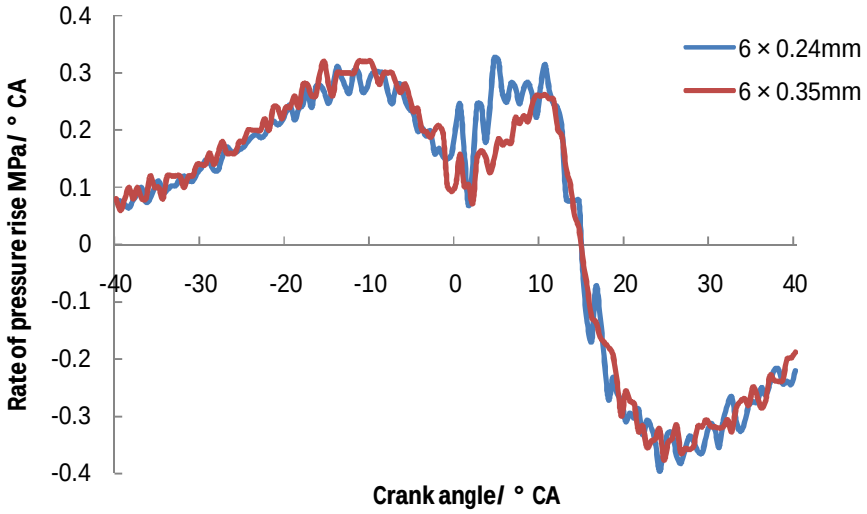

Fig. 12. Pressure rise rate for different orifice diameters at 1400 r/min rotation speed

4. Conclusion

The main content of this thesis is to study the effect of different orifice diameters on the combustion and emission of biodiesel supercharged engine.

(1) At a certain rotational speed, CO, HC, carbon smoke emissions are small and NOx emissions are large for orifice diameter 6×0.24mm. The CO, HC, and carbon smoke emissions are large and NOx emissions are small for the orifice diameter of 6×0.35mm.

(2) When the rotational speed is certain, the nozzle diameter 6 × 0.24mm of the cylinder pressure, heat release rate, pressure rise rate peak are higher than the nozzle diameter 6 × 0.35mm, the phase of the two types of nozzles is very close. Before the emergence of the peak, the cylinder pressure of the orifice diameter 6 × 0.35 mm is large and the heat release rate is small, and after the peak, the difference between the cylinder pressure and heat release rate is not obvious. The pressure increase rate of the two types of nozzles have two peaks, the first peak value is basically overlap, the different diameter of the nozzle mainly affects the second peak, the peak of the nozzle diameter 6 × 0.24mm is high, and the difference is not obvious after the second peak.

Disclaimer (Artificial intelligence)

Option 1:

Author(s) hereby declare that NO generative AI technologies such as Large Language Models (ChatGPT, COPILOT, etc) and text-to-image generators have been used during writing or editing of manuscripts.

References

[1]Eric Evans Osei Opoku, et al."Energy innovation investment and renewable energy in OECD countries."Energy Strategy Reviews 54.(2024):101462-101462.
[2]Kanchan Kumar Sen, et al."Clarifying the linkage between renewable energy deployment and energy justice: Toward equitable sustainability."Sustainable Futures 8.(2024):100236-100236.
[3]Yolcan, Oguz Ozan. "World energy outlook and state of renewable energy: 10-Year evaluation." Innovation and Green Development 2.4 (2023): 100070.
[4]Ahmad, Fayyaz, et al. "Natural resources and environmental quality: Exploring the regional variations among Chinese provinces with a novel approach." Resources Policy 77 (2022): 102745.
[5]Aleixandre-Tudó, José Luis, et al. "Renewable energies: Worldwide trends in research, funding and international collaboration." Renewable energy 139 (2019): 268-278.
[6]Ansari, Mohd Arshad, Salman Haider, and Tariq Masood. "Do renewable energy and globalization enhance ecological footprint: an analysis of top renewable energy countries?." Environmental Science and Pollution Research 28.6 (2021): 6719-6732.
[7]Jebli, Mehdi Ben, and Slim Ben Youssef. "Output, renewable and non-renewable energy consumption and international trade: Evidence from a panel of 69 countries." Renewable energy 83 (2015): 799-808.
[8]Fraser, Timothy, Andrew J. Chapman, and Yosuke Shigetomi. "Leapfrogging or lagging? Drivers of social equity from renewable energy transitions globally." Energy Research & Social Science 98 (2023): 103006.
[9]Cheng, Xuanmei, et al. "Dual carbon goals and renewable energy innovations." Research in International Business and Finance (2024): 102406.
[10]ur Rehman, Anis, et al. "Multifaceted Impacts of Widespread Renewable Energy Integration on Socio-Economic, Ecological, and Regional Development." Sustainable Futures (2024): 100241.
[11]Wang, Ya**g, et al. "A comprehensive review of exergy analysis in biodiesel-powered engines for sustainable power generation." Sustainable Energy Technologies and Assessments 68 (2024): 103869.
[12]Naylor, Rosamond L., and Matthew M. Higgins. "The rise in global biodiesel production: Implications for food security." Global food security 16 (2018): 75-84.
[13]Tamilvanan, A., et al. "Feasibility study on raw Simarouba glauca oil as an alternate fuel in a diesel engine and comparative assessment with its esterified oil." Fuel 327 (2022): 125168.
[14]Doğan, Battal, and Derviş Erol. "The investigation of energy and exergy analyses in compression ignition engines using diesel/biodiesel fuel blends-a review." Journal of Thermal Analysis and Calorimetry 148.5 (2023): 1765-1782.
[15]Demirbas, Ayhan. "Progress and recent trends in biodiesel fuels." Energy conversion and management 50.1 (2009): 14-34.
[16]Sedghi, Reza, et al. "Turning biodiesel glycerol into oxygenated fuel additives and their effects on the behavior of internal combustion engines: A comprehensive

systematic review." Renewable and Sustainable Energy Reviews 167 (2022): 112805.
[17]Wu, Guirong, Jun Cong Ge, and Nag Jung Choi. "A comprehensive review of the application characteristics of biodiesel blends in diesel engines." Applied Sciences 10.22 (2020): 8015.
[18]Chong, Cheng Tung, et al. "Biodiesel sustainability: The global impact of potential biodiesel production on the energy–water–food (EWF) nexus." Environmental Technology & Innovation 22 (2021): 101408.
[19]Dahake, Manoj, et al. "Intelligent Decision-Based Hydrogen-Biodiesel engine to improve engine performance." Fuel 367 (2024): 131449.
[20]Lv, Yonggang, et al. "Investigation of biodiesel and its blends fueled diesel engine: An evaluation of the comprehensive performance of diesel engines." Renewable Energy (2024): 120918.
[21]Khalaf, Mohamed, et al. "A comparative study of diesel engine fueled by Jatropha and Castor biodiesel: Performance, emissions, and sustainability assessment." Process Safety and Environmental Protection 188 (2024): 453-466.
[22]Rajpoot, Aman Singh, et al. "Comparative analysis of energy, exergy, emission, and sustainability aspects of third generation microalgae biodiesels in a diesel engine." Process Safety and Environmental Protection 188 (2024): 1026-1036.
[23]Youssef, Abdulkarim, and Amr Ibrahim. "An experimental evaluation for the performance of a single cylinder CI engine fueled by a Diesel-Biodiesel blend with alcohols and Zinc-Aluminate nanoparticles as additives." Materials Today: Proceedings (2024).
[24]Sengupta, Anindita, et al. "Enhancing Combustion Stability in Biodiesel Engines: The Plausibility of n-Butanol Injection Phasing and Reactivity-Controlled Compression Ignition–An Experimental Endeavour." Fuel 371 (2024): 131978.
[25]Ergen, Gokhan. "Comprehensive analysis of the effects of alternative fuels on diesel engine performance combustion and exhaust emissions: Role of biodiesel, diethyl ether, and EGR." Thermal Science and Engineering Progress 47 (2024): 102307.
[26]Doppalapudi, Arun Teja, Abul Kalam Azad, and M. M. K. Khan. "Experimental investigation on diesel engine performance, combustion, and emissions characteristics with Tucuma and Ungurahui biodiesel blends." Fuel 371 (2024): 132161.
[27]Asaad, Sara Maen, et al. "Response surface methodology in biodiesel production and engine performance assessment." International Journal of Thermofluids (2023): 100551.
[28]Li, Yuqiang, et al. "Stratified premixed combustion optimization of a natural gas/biodiesel dual direct injection engine." Energy 294 (2024): 130935.
[29]Jaiganesh, Jayapal, R. Prakash, and M. Gowthama Krishnan. "Exploring the synergistic potential of prosopis juliflora and waste plastic oil biodiesel through investigation of performance, combustion, and emission in a CRDI engine: A shift towards sustainable fuel." Process Safety and Environmental Protection 184 (2024): 720-735.
[30]Xu, Leilei, et al. "Large eddy simulation of spray and combustion characteristics of biodiesel and biodiesel/butanol blend fuels in internal combustion

engines." Applications in Energy and Combustion Science 16 (2023): 100197.
[31]Ameresh, Hiremat, Gadepalli Ravi Kiran Sastry, and Jibitesh Kumar Panda. "A novel experimental performance and emission study on CRDI engine using hydrogenated and green biodiesels: A turbo powered engine with hydrogen dual fuel and ANN prediction approach." Fuel 363 (2024): 130963.